How to cite: Demir, V. & H. Yürdem, 2025. Investigation of local pressure losses in reducers for sprinkler irrigation systems: Experimental, analytical and CFD approaches. Ege Univ. Ziraat Fak. Derg., 62 (4): 435-449, https://doi.org/10.20289/zfdergi.1623449

Research Article
(Araştırma Makalesi)

Vedat DEMİR[1*]

Hüseyin YÜRDEM[1]

[1]Ege University, Faculty of Agriculture, Department of Agricultural Engineering and Technologies, 35100, Bornova, İzmir, Türkiye

* Corresponding author (Sorumlu yazar):
vedat.demir@ege.edu.tr

Keywords: CFD, conical contraction, fitting, local friction loss, minor pressure loss, reduction

Anahtar sözcükler: HAD, konik daralma, ekleme parçası, lokal sürtünme kaybı, yerel basınç kaybı, redüksiyon

Ege Üniv. Ziraat Fak. Derg., 2025, 62 (4):435-449
https://doi.org/10.20289/zfdergi.1623449

Investigation of local pressure losses in reducers for sprinkler irrigation systems: Experimental, analytical and CFD approaches

Yağmurlama sulama sistemlerinde kullanılan redüksiyonlarda basınç kayıplarının incelenmesi: Deneysel, sayısal ve CFD yaklaşımlarıyla

Received (Alınış): **08.03.2025** **Accepted** (Kabul Tarihi):**18.06.2025**

ABSTRACT

Objective: This study aims to investigate the local pressure losses for conical reducers used in sprinkler irrigation systems using experimental, analytical, and Computational Fluid Dynamics (CFD) methods.

Material and Methods: Eight different reducers with nominal outer diameters of 90-75, 110-90, and 110-75 mm were considered. In the experiments, the pressure losses in the reducers were measured at different water flow rates. The CFD analysis was carried out using the Realizable k-ε, SST k-ω, and RSM turbulence models. The pressure loss coefficients were determined by measurements, analytically, and CFD analysis and were compared with each other.

Results: Taking the experimental data into account, the local loss coefficients for the $R1_{90-75}$, $R2_{90-75}$, $R4_{110-90}$, and $R5_{110-90}$, reducers were determined to be values between 0.5 and 1.0. The $R6_{110-75}$, and $R7_{110-75}$, $R8_{110-75}$ reducers local loss coefficients between 0.8 and 1.5 were determined. The local loss coefficients determined using the SST k-ω turbulence model considered in the CFD analysis were in better agreement with the experimental results.

Conclusion: It can be said that the pressure losses in the newly designed reducers could be determined by the CFD analysis at the design stage, and it would be useful to use these values in the system design.

ÖZ

Amaç: Çalışmada, yağmurlama sulama sistemlerinde kullanılan redüksiyonlar için yerel basınç kayıplarının deneysel, analitik ve Hesaplamalı Akışkanlar Dinamiği (CFD) yöntemleri ile incelenmesi amaçlanmıştır.

Materyal ve Yöntem: Çalışmada, nominal dış çapları 90-75, 110-90 ve 110-75 mm olan sekiz farklı redüksiyon dikkate alınmıştır. Denemelerde, redüksiyonlardaki basınç kayıpları farklı su geçiş debilerinde ölçülmüştür. Redüksiyonlardaki basınç kayıpları, teorik eşitliklerle ve Reliazable k-ε, SST k-ω ve RSM türbülans modelleri dikkate alınarak CFD analiz yöntemiyle incelenmiştir.

Araştırma Bulguları: Deneysel veriler dikkate alındığında yerel kayıp katsayıları, $R1_{90-75}$, $R2_{90-75}$, $R4_{110-90}$, $R5_{110-90}$ redüksiyonları için 0.5 ile 1.0 arasında ve $R6_{110-75}$, $R7_{110-75}$, $R8_{110-75}$ redüksiyonları için ise 0.8 ile 1.5 arasında belirlenmiştir. Sayısal analiz yönteminde SST k-ω türbülans modeli kullanılarak belirlenen yerel kayıp katsayıları, deneysel sonuçlar ile en iyi uyumu göstermiştir.

Sonuç: Yeni tasarlanan redüksiyonlardaki basınç kayıplarının tasarım aşamasında sayısal analiz yöntemi ile belirlenebileceği ve sistem tasarımında kullanılmasının uygun olacağı söylenebilir.

INTRODUCTION

Sprinkler irrigation is a method of controlled application of water similar to rainfall. The water is distributed under pressure through a network that can consist of pumps, valves, main and/or sub-main pipes, laterals, and sprinklers. The success of a sprinkler irrigation system depends on the selection of the appropriate sprinkler type and its components, the hydraulic design of the system, and its operation at suitable operating pressures.

Pressure loss due to friction is important parameters in the hydraulic design of the sprinkler irrigation system. The main factors affecting pressure losses are the type of pipe, the type of flow in the pipe, and its geometric dimensions that cause a change in the direction or cross-section of the flow in the pipeline. Reducers, which are usually made of polyethylene (PE), are used to connect pipes with different diameters in sprinkler irrigation systems. These conical contraction parts interrupt a uniform flow, causing turbulence and thus additional losses. These additional losses are generally lower than the pressure losses in long pipe networks. However, the local losses in irrigation networks consisting of short pipes and many fittings can be higher than the losses in straight pipes. Therefore it is important to take local losses into account when designing the system (Idel'chik, 1960; Daugherty & Franzini, 1965; Cengel & Cimbala, 2006).

The pressure losses in the flow at the fittings can be calculated using the coefficients given in the literature. However, these coefficients are constant and cannot take into account the properties of the flow. Essentially, the pressure losses in the flow in pipes and fittings are a function of the Reynolds number. Therefore, parameters such as flow velocity, pipe diameter, and roughness have a direct effect on the loss coefficient. For instance: radius of curvature at elbows; and sudden or gradual contraction or expansion at reducers. Several experimental studies have been carried out on total friction and local losses for different types of irrigation parts. Most studies focus on the pipes and emitters used in drip irrigation systems (Howell & Barinas, 1980; Bagarello et al., 1997; Juana et al., 2002; Provenzano & Pumo, 2004; Demir et al., 2019). Experimental studies on components of sprinkler irrigation systems are quite limited.

Computational Fluid Dynamics (CFD) is a method of modeling flow patterns using advanced algorithms and computers. CFD enables engineers to make faster and better decisions to improve the quality, durability, and performance of their designs. The studies carried out using the CFD method for the fittings in the fluid lines mainly focused on valves and elbows (Cürebal, 2016). In addition, several studies have been conducted on the design of filters, emitters, and jet sprayers for micro irrigation systems around the world (Palau-Salvador et al., 2004; Wei et al., 2006; Zhang et al., 2007; Wang et al., 2009; Demir et al., 2020; Demir et al., 2022). Saldivia et al. (1990) modeled pressure losses using the finite element method with a similar approach for equivalent pipe lengths in different system components of sprinkler irrigation systems. Various researchers have conducted studies on the gradual expansion (Choi et al., 2019), and contraction (Deev et al., 2009; Satish et al., 2013; Tan et al., 2013; Narayane et al., 2014; Das et al., 2015; Jivani & Naik, 2019), particularly using the CFD approach. The researchers performed CFD analyses at specific velocities for constant expansion or contraction angles and used k-epsilon (k-ε), k-omega (k-ω), and Reynolds stress model (RSM) turbulence models for their analyses. The CFD results were compared with the results of the analytical method, and it was found that the local loss coefficients change depending on the Reynolds number. No experimental and/or simulation-based studies were found on reducers with diameters used in sprinkler irrigation systems.

This study aims to determine the local pressure losses for conical reducers used in sprinkler irrigation systems using experimental, analytical, and computational fluid dynamics (CFD) methods.

MATERIALS and METHODS

The study considered eight different PE (polyethylene) reducers from different companies that are widely used in sprinkler irrigation systems. The reducers were categorized into three groups; they were used in the flow transition between nominal diameters of 90 mm and 75 mm, 110 mm and 90 mm, and 110 mm and 75 mm. Details of the reducers are given in Figure 1 and Table 1.

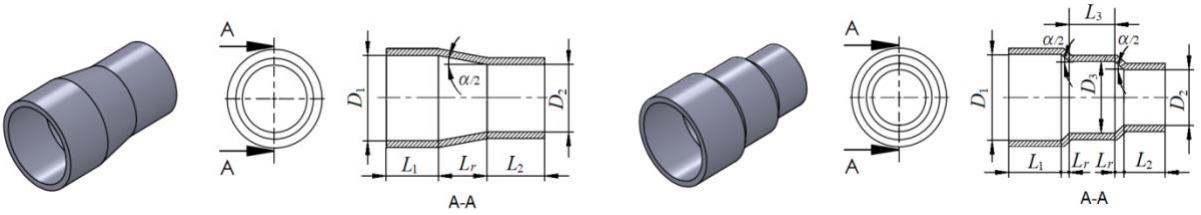

Figure 1. General view of the reducers used in the study.

Şekil 1. *Çalışmada ele alınan redüksiyonların genel görünüşleri.*

Table 1. Technical data of the reducers used in the study

Çizelge 1*. Çalışmada ele alınan redüksiyonların teknik özellikleri*

Types of reducers	D_1 (mm)	D_2 (mm)	D_3 (mm)	$\alpha/2$	L_r (mm)	L_1 (mm)	L_2 (mm)	L_3 (mm)
$R1_{90\text{-}75}$	75	63	-	7°	48.9	64	48	-
$R2_{90\text{-}75}$	77	63	-	17°	22.9	77	62	-
$R3_{90\text{-}75}$	69	65	-	15°	7.5	64	48	-
$R4_{110\text{-}90}$	94	75	-	10°	53.9	61	66	-
$R5_{110\text{-}90}$	95	75	-	18°	30.8	72	62	-
$R6_{110\text{-}75}$	96	63	-	20°	45.3	67	58	-
$R7_{110\text{-}75}$	94	64	-	35°	21.4	67	62	-
$R8_{110\text{-}75}$	96	62	80	41°	9.8	61	48	53

The study was carried out in three stages: experimental, analytical, and CFD analysis.

Experimental studies

In the first step of the study, experiments were carried out in the Pump and Irrigation Equipment Test Laboratory of the Department of Agricultural Engineering and Technologies at the Faculty of Agriculture at Ege University and the experimental setup was shown in Figure 1. The experimental apparatus was used to determine the pressure loss caused by the reducers with different diameters at different flow rates.

The water was supplied by a submersible pump, and the flow rate was controlled by a valve during the experiments. The flow rate was measured with an electromagnetic flow meter (Emd-C100F type DN100, Bass-Ela, Czech Republic) with an accuracy of ±0.5% (±0.4 L/s). The pressures at different flow rates were measured with two pressure sensors (PAA-21 SR type, Keller, Switzerland) with an accuracy of ±0.2% (±1.2 kPa) when the flow was stabilized.

As stated in various references when measuring pressure drops in the fittings, to minimize turbulence interaction, it is recommended that the pressure measurements at the inlet and outlet of the fitting should be far from at least 5 or 10 times the inner diameter of the pipe and not less than 1 m from the inlet and outlet of the fittings (ASAE, 2003; Cengel & Cimbala, 2006; Ntengwe et al., 2015; TS, 2019). In the study, the measuring distance for the reducer with the largest inner diameter is 10x96=960 mm. For this reason, the pressure sensors used in the study were placed 1 m before and after all the reducers to conduct the studies under the same conditions.

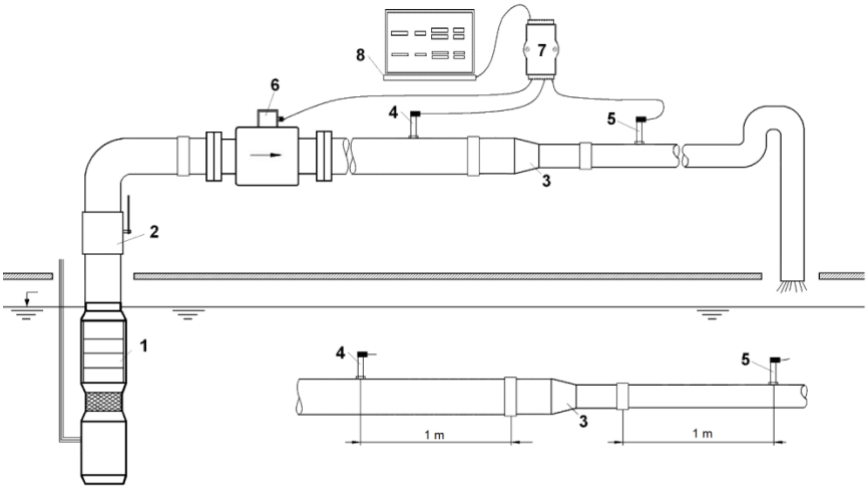

Figure 2. Schematic representation of the experimental apparatus: (1) submersible pump and water inlet pipe; (2) control valve; (3) reducer; (4) inlet pressure sensor; (5) outlet pressure sensor; (6) electromagnetic flow meter; (7) data acquisition system; (8) computer.

Şekil 2. *Deneme düzeninin şematik görünümü: (1) dalgıç pompa ve su giriş borusu; (2) kontrol vanaları; (3) redüksiyon; (4) giriş basınç sensörü; (5) çıkış basınç sensörü; (6) manyetik debimetre; (7) veri algılama-kayıt sistemi; (8) bilgisayar.*

Measurements were recorded by a data acquisition system (ADAM 4520 and ADAM 4017+, Advantech Automation Corp., USA) using GeniDAQ version 4.25 data acquisition software. The data acquisition system used in this study can record 6 data per second. The data was recorded for 15 seconds in the study. During the entire measurement period, 15x6=90 flow and pressure values were recorded separately and the average values were used for the study. During the experiments, the water temperature was measured with a digital thermometer, and it varied between 18 and 22°C. The pressure losses in straight PE pipes and reducers were measured repeatedly.

Analytical studies

In the second step of the study, comparative calculations were carried out using theoretical equations. The pressure loss (ΔP_f) in the straight PE pipes at the inlet and outlet of the reducer was calculated using the Darcy-Weisbach equation (White, 2001; Munson et al., 2002; Cengel & Cimbala, 2006).

$$\Delta P_f = f \frac{L}{D} \frac{\rho V^2}{2} \quad (1)$$

The Darcy-Weisbach friction factor (f) for a fully developed turbulent flow in a straight pipe was calculated taking into account the relative roughness (ε/D) and the Reynolds number (Re) and using the following equations (Cengel & Cimbala, 2006);

$$\frac{1}{\sqrt{f}} = -1.8\, log\left[\frac{6.9}{Re} + \left(\frac{\varepsilon/D}{3.7}\right)^{1.11}\right] \quad (2)$$

$$Re = \frac{VD}{\nu} \quad (3)$$

where: ΔP_f is the pressure loss in a straight pipe in Pa; V is the mean flow velocity in the pipe in ms^{-1}; D is the inner diameter of the pipe in m; L is the pipe length in m; ρ is the density of water in kgm^{-3}; f is the Darcy-Weisbach friction factor; ε is the roughness of the inner surface of a pipe in m; ν is the kinematic viscosity of water m^2s^{-1} (ν=1.01×10^{-6} m^2s^{-1} for 20°C).

The local pressure loss (ΔP_k) for each reducer was determined by subtracting the calculated pressure losses for the straight PE pipe from the measured total pressure losses. In addition, the local loss coefficients (k) at different flow velocities ($V=4Q/\pi D^2$) were calculated using Equation (4).

$$\Delta P_k = k\frac{\rho V^2}{2} \qquad \Rightarrow \qquad k = \frac{\Delta P_k}{\frac{1}{2}\rho V^2} \tag{4}$$

These data were used to determine the relationships between the flow rate and the pressure loss, as well as the flow velocity and the local loss coefficient. In addition, comparisons were made with the equations and coefficients given in the literature for conical contraction fittings. The theory used for this purpose is explained below.

The total local pressure loss in the tapered flow includes the losses in the transition region between the fully developed inlet and outlet flows (Figure 3). The equation for the local pressure loss in this region is expressed in Equation (5) (Rennels & Hudson, 2012).

$$hk = k\frac{V_2^2}{2g} = k_{acc}\frac{V_C^2}{2g} + \frac{(V_C - V_2)^2}{2g} \tag{5}$$

where: hk is the total local pressure loss in m; Vc is the mean flow velocity in the vena contracta region in ms^{-1}; V_2 is the mean flow velocity in the pipe outlet in ms^{-1}; k_{acc} is the local loss coefficient for the acceleration part of the flow in the conical region. In the equation, the first and second terms express the gradual acceleration of the flow towards the vena contracta region and the sudden expansion of the flow from the vena contracta to the outflow, respectively.

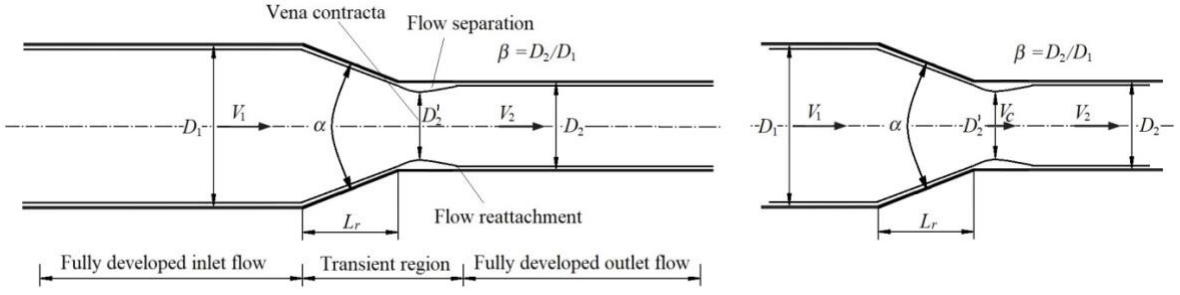

Figure 3. Flow in conical contraction (Rennels & Hudson, 2012).

Şekil 3. *Konik daralmada akış (Rennels & Hudson, 2012).*

Crane (1982) and Rennels & Hudson (2012) summarized the experimental data for the local loss coefficients of such conical pipe transitions and stated that they can be determined by semi-empirical equations. There is an acceleration in the transition region due to the contraction along the flow channel and a deceleration in the outlet pipe due to the expansion of the flow separation and confluence regions. The region with the smallest flow cross-section in the separation region of the outlet is called the vena contracta, and the velocity is highest in this region. Depending on these flow characteristics, the pressure losses in the transition region are expressed as the sum of the local pressure losses due to the surface friction in the conical contraction region and the contraction that occurs at the transition from the conical to the expansion region, Equation (6) (Roul & Dash, 2011; Rennels & Hudson, 2012).

$$hk = hk_{fr} + hk_{con} \tag{6}$$

where: hk_{fr} is the local pressure loss due to surface friction in the conical contraction region in m; hk_{con} is the contraction pressure loss that occurs at the transition from the conical to the expansion region in m. The researchers found that the pressure losses due to surface friction can be significant due to the increase in surface length at a small angle. The pressure losses for surface friction and conical contractions can be calculated using Equations (7) and (8) (Rennels & Hudson, 2012).

$$hk_{fr} = k_{fr}\frac{V_2^2}{2g} \quad (7)$$

$$hk_{con} = k_{con}\frac{V_2^2}{2g} \quad (8)$$

The local loss coefficients for surface friction (k_{fr}), conical contraction (k_{con}), and total coefficient (k) in the equations were calculated using the following equations:

$$k_{fr} = \frac{f\,(1-\beta^4)}{8\,sin\,(\alpha/2)} \quad (9)$$

$$k_{con} = 0.0696\,sin\,(\alpha/2)\,(1-\beta^5)\lambda^2 + (\lambda-1)^2 \quad (10)$$

$$\lambda = 1 + 0.622(\alpha/180)^{4/5}(1-0.215\beta^2-0.785\beta^5) \quad (11)$$

$$k = k_{fr} + k_{con} \quad (12)$$

where: $\beta=D_2/D_1$ diameter ratio; λ is the rate of velocity in the contraction jet; α is the conical contraction angle. The mean flow velocity (V_c) in the vena contracta region was calculated using the ratio of the velocity in the contraction jet according to Equation (13), and the local loss coefficient (k) was calculated according to Equation (14).

$$\lambda = \frac{V_c}{V_2} \quad \Rightarrow \quad V_c = \lambda \cdot V_2 \quad (13)$$

$$hk = k\frac{V_c^2}{2g} \quad \Rightarrow \quad k = \frac{2ghk}{V_c^2} = \frac{\Delta P}{\frac{1}{2}\rho V_c^2} \quad (14)$$

The friction factor (f) depends on the relative roughness of the conical surface, the hydraulic diameter at the cone outlet, and the Reynolds number. The local loss coefficient for conical contractions is a function of the diameter ratio ($\beta=D_2/D_1$), the cone contraction angle (α), and the ratio of velocity in the contraction jet (λ). Equations (15) and (16), which are often used as a function of the contraction angle (α) in the calculation of the local loss coefficients for conical contractions, were taken into account in the comparison (Crane, 1982).

$$k = \frac{0.8\,sin\,(\alpha/2)\,(1-\beta^2)}{\beta^4} \qquad \alpha \le 45^o \quad (15)$$

$$k = \frac{0.5\,(1-\beta^2)\sqrt{sin(\alpha/2)}}{\beta^4} \quad 45^o < \alpha \le 180^o \quad (16)$$

In addition to the measurement results for the reducers, the pressure losses and the local loss coefficients were calculated using the theoretical equations given by Rennels and Hudson (2012) and Crane (1982). Furthermore, the local loss coefficients were calculated as a function of the velocity in the region of the vena contracta, and their variations were shown for each reducer.

CFD analysis

In the third step of the study, the pressure losses in the reducers were investigated by CFD analysis using ANSYS Fluent 17.2 software (ANSYS, 2016). Each reducer was modeled and meshed for the flow analysis (Figure 4). The mesh structure was divided into three sections: Inlet pipe, outlet pipe, and reducer. In the preliminary studies conducted to determine the most appropriate number of elements

for the solution, different network structures and different numbers of elements were created in different regions. By increasing the number of elements, the optimal network structure were performed. The hexahedral mesh structure was used for the analysis. The maximum dimension of a grid in the mesh structure was set to be 2 mm in the reducer section and 5 mm in the inlet and outlet pipes. In addition, the pipe walls were provided with 10 layers. The number of nodes and elements in this mesh structure was more than 4.1×10^5 and 3.7×10^5, respectively.

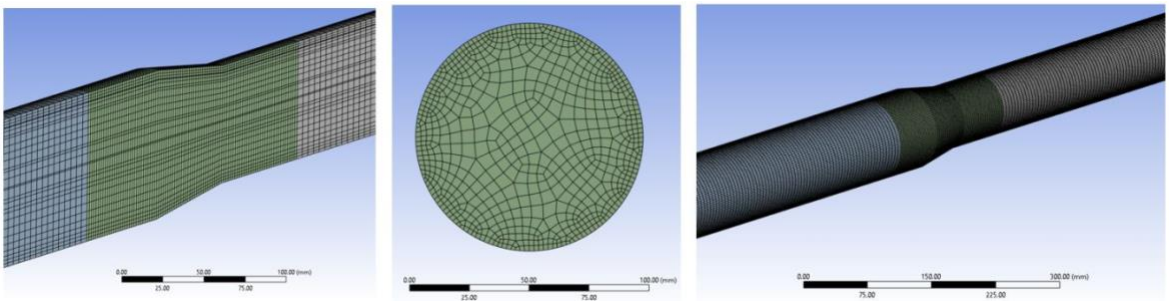

Figure 4 Geometry and mesh structure of the test pipes and the reducer.

Şekil 4. *Redüksiyon ve deneme borusunun geometrisi ve ağ yapısı.*

The turbulence models and options considered in the study are given below:

- Realizable k-ε turbulence model with standard wall and curvature correction options,
- SST k-ω turbulence model with low-Re corrections, corner flow correction, and production limiter options,
- LPS RSM (Reynolds Stress Model) turbulence model with wall BC from the k-equation, wall reflection effects, and standard wall options.

For the CFD analysis, water was chosen as the fluid. It was assumed that the fluid is steady, incompressible, viscous, and without gravity. Coupled algorithms and second-order discretization schemes were used for all solutions. The absolute roughness of PE pipes is often neglected or considered too low. However, since the reducers are friction-welded, the weld zones contain too much roughness. Therefore, the level of surface roughness was assumed to be 0.1 mm in the pipe section and 0.5 mm in the reducer.

The measured flow rates at the pipe inlet and the measured pressures at the pipe outlet were defined by the inlet and outlet boundary conditions, respectively. The convergence accuracy of the solution was assumed to be 1×10^{-10}.

Statistical analysis

The mean absolute error (MAE) and root mean square error (RMSE) were used to compare the differences between the experimental pressure loss data and the data predicted by CFD models (Willmott et al., 1985; Willmott & Matsuura, 2005).

$$MAE = \frac{1}{n}\sum_{i=1}^{n}\left|\Delta P_{i,exp} - \Delta P_{i,CFD}\right| \quad (17)$$

$$RMSE = \left[\frac{1}{n}\sum_{i=1}^{n}\left(\Delta P_{i,exp} - \Delta P_{i,CFD}\right)^2\right]^{1/2} \quad (18)$$

where: $\Delta P_{i,exp}$ is experimental and $\Delta P_{i,CFD}$ is the simulation values, n is the number of data.

The lowest value of these comparison criteria represents the highest estimate of the model.

RESULTS and DISCUSSION

The experimental results of the measured pressure loss at different flow rates for eight different reducers and the calculated Reynolds numbers and local loss coefficients for the outlet pipe are shown in Table 2. The variations of the local loss coefficient as a function of the outlet velocity are shown in Figure 5.

Table 2. Pressure losses and local loss coefficients in the reducers

Çizelge 2*. Redüksiyonlarda basınç kayıpları ve kayıp katsayıları*

Types of reducers	Flow rate Q (Ls^{-1})	Reynolds number Re^*	Pressure loss in reducer ΔP_k (kPa)	Local loss coefficient for reducer k^*
$R1_{90\text{-}75}$	6.8-15.7	162201-374055	2.26-8.60	0.68-0.95
$R2_{90\text{-}75}$	5.6-15.5	136959-380631	1.38-7.95	0.64-0.86
$R3_{90\text{-}75}$	6.7-15.7	138752-322993	1.32-5.29	0.47-0.64
$R4_{110\text{-}90}$	7.6-15.8	159836-333723	1.22-4.55	0.71-0.83
$R5_{110\text{-}90}$	5.2-15.8	110649-337274	0.72-4.58	0.71-1.05
$R6_{110\text{-}75}$	4.3-16.0	130926-488959	1.40-12.74	0.96-1.48
$R7_{110\text{-}75}$	4.8-15.9	139902-459907	1.53-12.14	0.99-1.35
$R8_{110\text{-}75}$	5.3-15.9	167120-500922	2.36-13.92	1.00-1.52

* The Reynolds numbers and local loss coefficients were calculated for the outlet pipe.

It can be seen that the pressure losses are between 0.72 and 8.6 kPa for single-stage reducers with nominal diameters of 90-75 and 110-90 mm and between 1.4 kPa and 13.92 kPa for two-stage reducers with nominal diameters of 110-75 mm (Table 2).

When Table 2 and Figure 5 are examined, it is seen that the local loss coefficients of all reducers used in the study vary depending on the velocity of the water in the pipeline. It can be seen that the local loss coefficients for single-stage reducers with different diameters are close to each other and that the local loss coefficients for two-stage reducers are higher than these values. The local loss coefficients were between 0.5 and 1.0 for single-stage reducers and between 1.0 and 1.5 for two-stage reducers.

The experimental results of the total pressure loss for all reducers were compared with the results of the CFD analysis performed with different turbulence models. The results are shown in Figure 6.

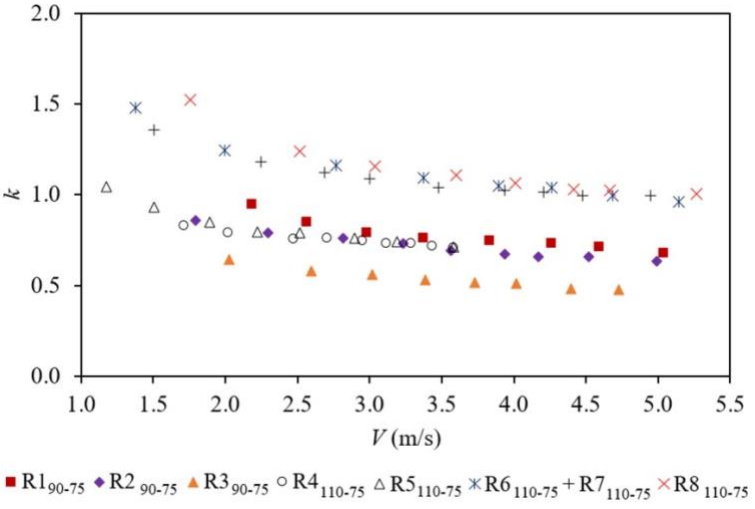

Figure 5. Variations of the coefficient of local loss as a function of the outlet velocity in the reducers.

Şekil 5. *Redüksiyonlarda kayıp katsayılarının çıkış hızına göre değişimleri.*

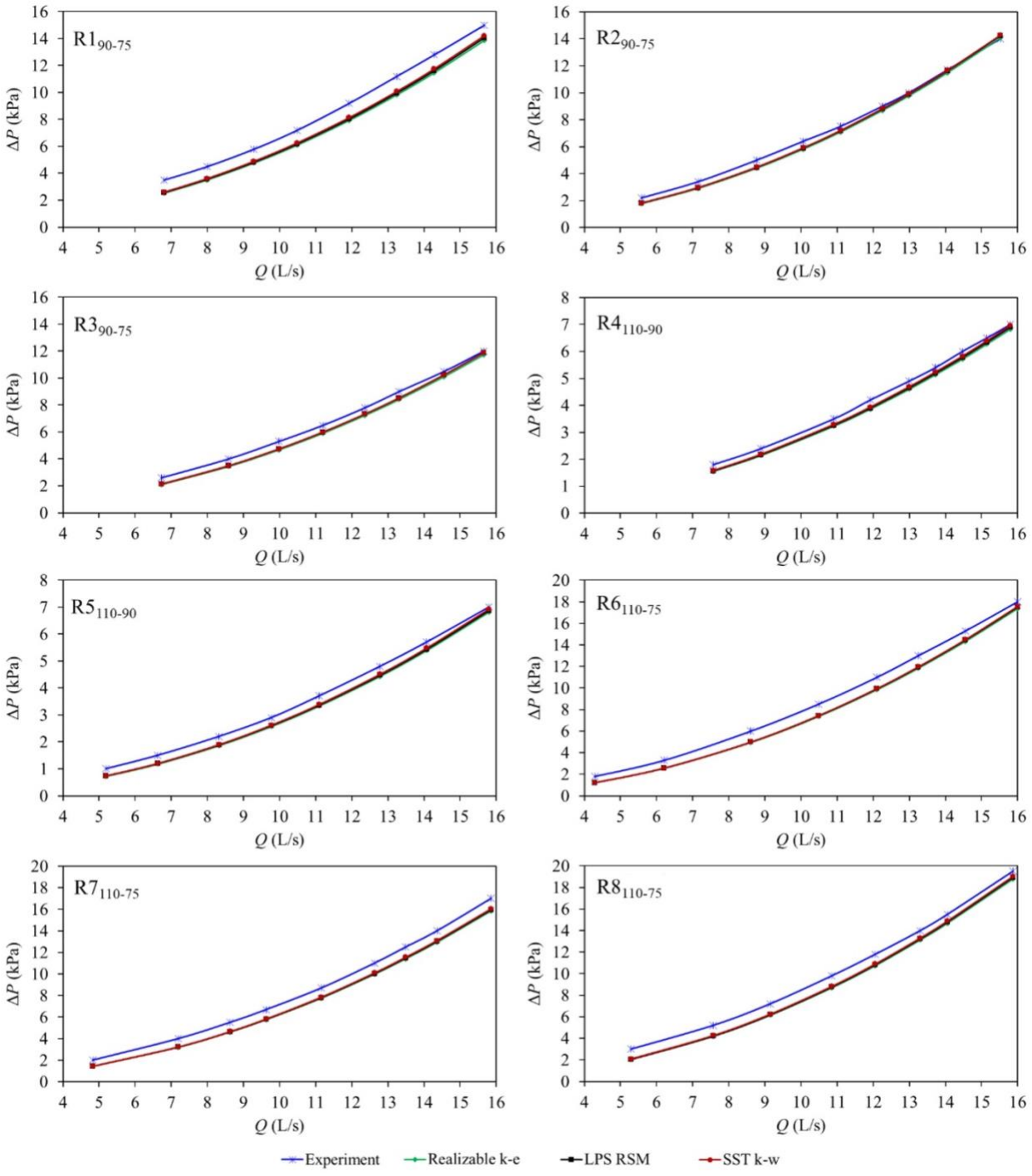

Figure 6. Comparison of the results of the total pressure loss with the experimental and the CFD analysis in reducers.

Şekil 6. *Redüksiyonlarda deneysel ve CFD analiz sonucu bulunan toplam basınç kaybı değerlerinin karşılaştırılması*

It was found that the local pressure losses for the reducers $R1_{90-75}$, $R2_{90-75}$, and $R3_{90-75}$ are quite close to each other (Figure 6). For the $R4_{110-90}$ and $R5_{110-90}$ reducers, the local pressure losses were close to each other but lower than for the 90-75 mm reducers. The enlargement of the cross-section at the same flow velocity leads to lower pressure losses. The local pressure losses in the two-stage reducers ($R6_{110-75}$, $R7_{110-75}$, and $R8_{110-75}$) were found to be similar.

The local pressure losses calculated with different turbulence models using CFD analysis were found to be quite close to each other (Figure 6). When comparing the measurement and simulation results, it can be seen that the results for some reducers (such as $R2_{90-75}$, $R4_{110-90}$, and $R5_{110-90}$) are very close to each other, while there are differences for some reducers (such as $R1_{90-75}$ and $R7_{110-75}$). The 3D models created for the simulation are very smooth. However, the reducers are manufactured by joining the pipe connection heads using the friction welding technique. Therefore, very high roughness occurs in the welding zones of the reducers. In addition, the water passages in the actual reducers could have gaps. These could also cause different vortices during the water passage in the experiments. The differences between the experimental and simulation data could be explained by the different roughness of the welding zones in the reducers and the surfaces of the water flow zone as well as by the additional pressure losses caused by the vortices in the pipe connections. The statistical evaluation of the measured and calculated pressure losses with different CFD turbulence models is given in Table 3.

Table 3. Comparison of the MAE and RMSE values between the measured values and the values calculated with CFD turbulence models

Çizelge 3. *Redüksiyonlar için ölçülen ve farklı CFD türbülans modelleri ile hesaplanan basınç kayıplarının istatiksel olarak MAE ve RMSE değerleri yönüyle karşılaştırılması*

Types of reducers	MAE*			RMSE**		
	SST k-ω	Realizable k-ε	LPS RSM	SST k-ω	Realizable k-ε	LPS RSM
$R1_{90-75}$	0.953	1.152	1.061	0.958	1.162	1.067
$R2_{90-75}$	0.298	0.372	0.322	0.341	0.408	0.361
$R3_{90-75}$	0.424	0.510	0.429	0.445	0.522	0.451
$R4_{110-90}$	0.178	0.261	0.217	0.189	0.265	0.224
$R5_{110-90}$	0.248	0.309	0.279	0.259	0.314	0.286
$R6_{110-75}$	0.824	0.927	0.848	0.854	0.954	0.877
$R7_{110-75}$	0.838	0.947	0.885	0.847	0.962	0.896
$R8_{110-75}$	0.812	0.950	0.866	0.831	0.958	0.881

* Mean Absolute Error (Equation 17)
** Root Mean Square Error (Equation 18)

As can be seen in Table 3, the lowest MAE and RMSE values between the measured and CFD simulation models were found for the SST k-ω turbulence model. Although the graphs in Figure 6 do not show much difference between the other models considered, it can be seen that the SST k-ω model statistically provides a better estimate than other models. It can be said that this turbulence model should be preferred for the estimation of pressure losses in reducers. Cürebal (2016), investigated the three-dimensional solution of turbulent flow in elbows with different diameters at different flow rates for air, natural gas, and water and found that the SST k-ω turbulence model showed better agreement with the experimental results.

In the study, the local loss coefficients were calculated using Equation (4) from the pressure losses measured experimentally and calculated with the SST k-ω turbulence model. In addition, the local loss coefficients were calculated using Equation (12) from Rennels and Hudson (2012), Equation (15) from Crane (1982), and Equation (14) as a function of velocity in the vena contracta region. The changes as a function of flow velocity for each reducer are shown in Figure 7.

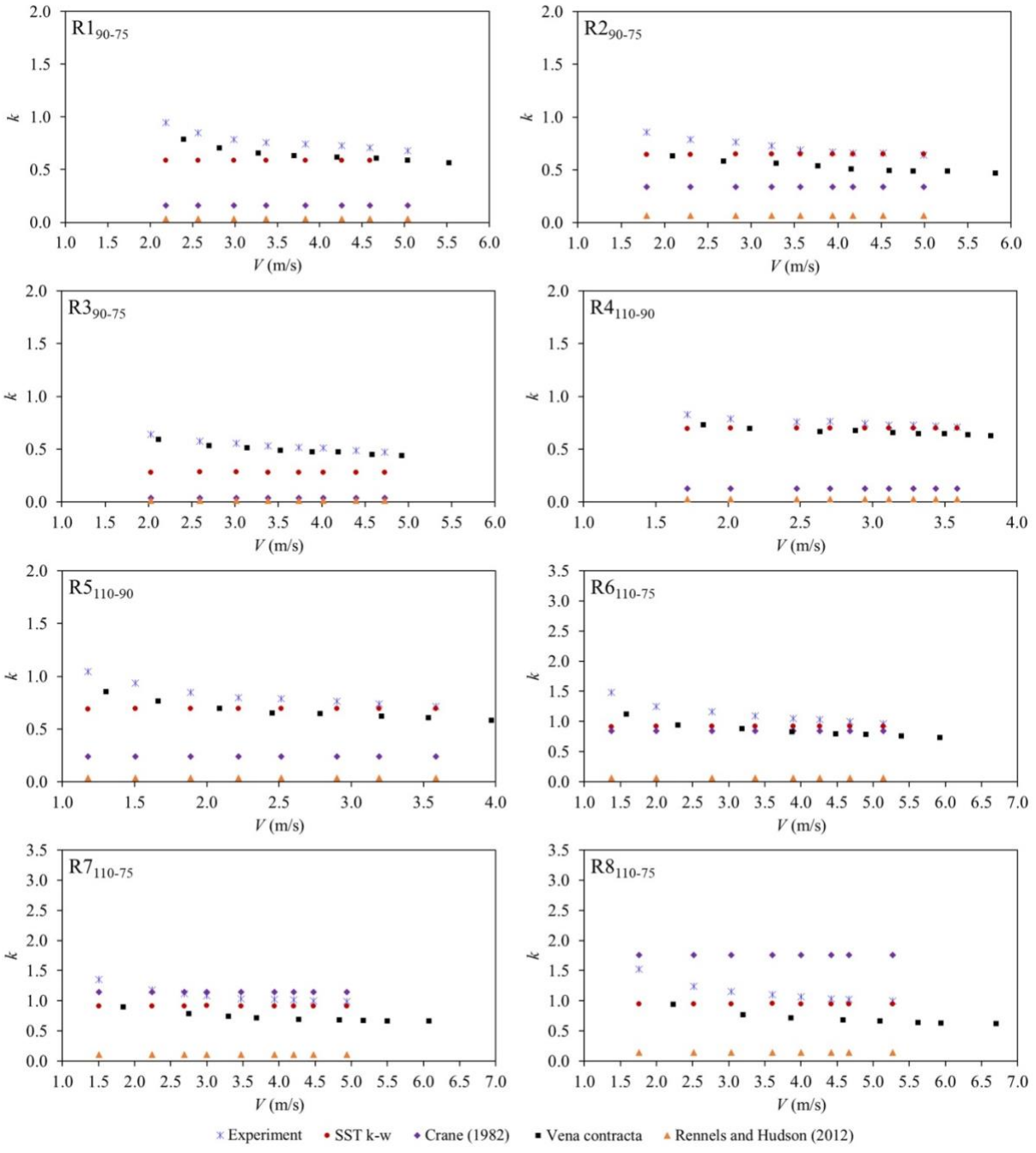

Figure 7. Comparison of the pressure loss coefficients in reducers determined by experimental and CFD analysis.

Şekil 7. *Redüksiyonlarda deneysel ve CFD analiz ile bulunan basınç kayıp katsayılarının karşılaştırılması.*

Figure 7 shows that the local loss coefficients calculated with the SST k-ω turbulence model and Equation (14) in the region of the vena contracta are close to each other for all reducers. The results of the CFD analysis of the reducers with different contraction angles using the SST k-ω turbulence model about the conical contraction and in particular, the flow in the region of the vena contracta are shown in Figure 8. The examination of Figure 8 shows that there are sudden pressure changes in the flow in the conical contraction of the reducers, and especially in the vena contracta, the pressure suddenly drops, and the turbulence intensity increases in this region.

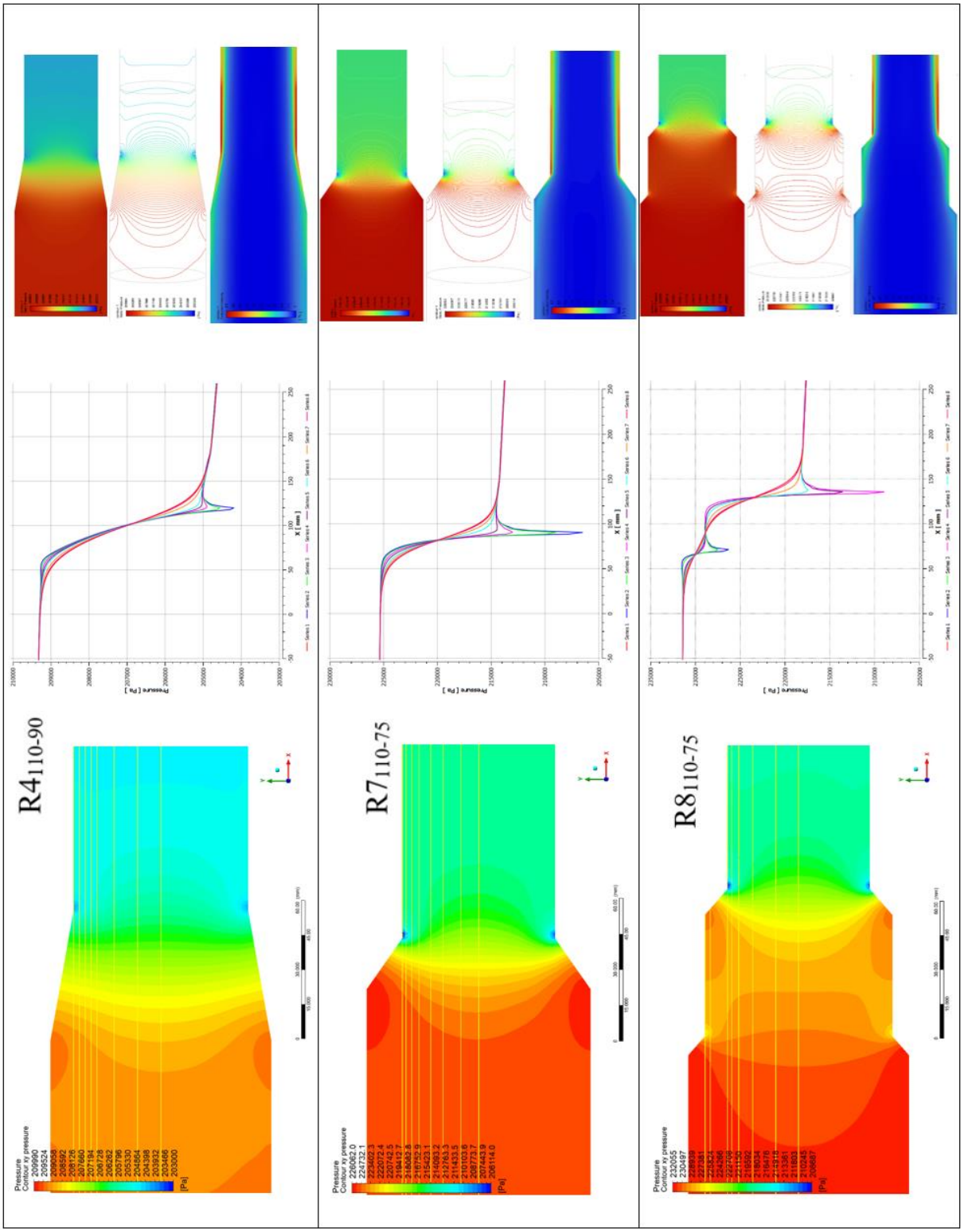

Figure 8. Flow analysis with the SST k-ω turbulence model in the region of the conical contraction and the vena contracta in reducers with different contraction angles.

Şekil 8. *Farklı* daralma *açılarına sahip redüksiyonlarda SST k-ω türbülans modeli ile konik daralma ve vena contracta bölgesinde akışın analizi*

When examining Figure 7, it is seen that the results obtained in the literature using the equations of Rennels and Hudson (2012) and Crane (1982) are different for the various reducers. In particular, the results calculated using the equation by Rennels and Hudson (2012) differ greatly from the measurement results. The results calculated using the equation by Crane (1982) show great variability from reducer to reducer. For example, while very low k-values were calculated for $R1_{90\text{-}75}$ and $R4_{110\text{-}90}$, very high k-values were calculated for $R8_{110\text{-}75}$. The reason for this could be that the k equation is calculated directly as a function of the contraction angle and other factors are not taken into account. For these reasons, it is clear that taking these two equations into account when calculating the pressure loss of the reducers used in irrigation systems could lead to errors for these nominal sizes. It can be seen that the equations (15 and 16) expressed by Crane (1982) for the local pressure loss coefficient are independent of the friction factor (*f*) and the Reynolds number (*Re*). Cengel and Cimbala (2006), stated that the local pressure loss coefficient calculated with these equations can be corrected with a coefficient of 1.05 for fully turbulent flows and 2.0 for fully developed laminar flows. However, as can be seen in Figure 7, the use of these coefficients for the turbulent flow region gave very different results from the experimental data for many of the reducers considered in the study.

The experimental results show that the local pressure loss coefficients in the single-stage reducers $R1_{90\text{-}75}$, $R2_{90\text{-}75}$, $R4_{110\text{-}90}$, and $R5_{110\text{-}90}$ are between 0.5 and 1.0, where 0.8 can be used as the average value for the calculations. For the two-stage reducers of types $R6_{110\text{-}75}$, $R7_{110\text{-}75}$, and $R8_{110\text{-}75}$ the local pressure loss coefficients vary between 0.8 and 1.5, whereby 1.2 can be used as an average value for the calculations.

CONCLUSION

The aim of this study is to determine the local pressure losses for conical reducers used in sprinkler irrigation systems using experimental, analytical, and CFD methods. Considering the experimental results, it was found that the local pressure loss coefficients for single-stage reducers with different diameters were close to each other. The local pressure loss coefficients were found between 0.5 and 1.0 for the single-stage reducers and between 0.8 and 1.5 for the two-stage reducers.

Realizable k-ε, SST k-ω, and LPS RSM turbulence models were considered in the study. It was found that the pressure losses calculated with all turbulence models were quite close to each other. The experimental local pressure losses were found to be slightly higher than the simulation results. This difference could be explained by the weld roughness in the manufacture of the reducer and the additional pressure losses caused by the vortices in the pipe connections.

The local pressure loss coefficients calculated with the theoretical equations for the reducers in the study were found to be quite different from the experimental and CFD simulation results. It was found that the local pressure loss coefficients calculated using the equation of Rennels and Hudson (2012) were quite different from the experimental results, while the equation of Crane (1982) showed a large variability from reducer to reducer. For these reasons, it can be said that using these two equations to calculate the local pressure loss coefficients for reducers can cause errors. When calculating the local pressure loss in the reducers with different CFD simulation models, it was found that the SST k-ω turbulence model was statistically closest to the experimental results.

Data Availability

Data will be made available upon reasonable request.

Author Contributions

Conception and design of the study: VD, HY; sample collection: VD, HY; analysis and interpretation of data: VD, HY; statistical analysis: VD, HY; visualization: VD, HY; writing manuscript: VD, HY.

Conflict of Interest

There is no conflict of interest between the authors in this study.

Ethical Statement

We declare that there is no need for an ethics committee for this research.

Financial Support

This study did not receive funding from any organization.

Article Description

This article was edited by Section Editor Dr. İkbal AYGÜN.

REFERENCES

ANSYS, 2016. Fluent theory guide R.17.2. Canonsburg, PA: ANSYS, Inc., 850 pp.

ASAE, 2003. Procedure for testing and reporting pressure losses in irrigation valves. ASAE S447, Feb03, ASAE Standards 2003: 941-943.

Bagarello, V., V. Ferro, G. Provenzano & D. Pumo, 1997. Evaluating pressure losses in drip-irrigation lines. Journal of Irrigation and Drainage Engineering, 123 (1): 1-7. https://doi.org/10.1061/(ASCE)0733-9437

Cengel, Y. A. & J. M. Cimbala, 2006. Fluid Mechanics: Fundamentals and Applications (1st edition). NY: McGraw-Hill, 940 pp.

Choi, S. H., S. Kim, J. Choi, J. T. Park & H. Jeong, 2019. Optimum angles of non-standard diffusers and reducers for engineering application. Journal of Mechanical Science and Technology, 33 (10): 4831-4841.

Crane, 1982. Flow of fluids through valves, fittings, and pipe. Joliet, IL: Metric Edition Crane Co, 133 pp.

Cürebal, T., 2016. Boru ekleme parçalarındaki akışın üç boyutlu incelenmesi. Karadeniz Teknik Üniversitesi, (Unpublished), Trabzon, 71 pp.

Das, P., M.M.K. Khan, M.G. Rasul & S. C. Saha, 2015. “Fluid flow characterictics on scale deposition in a concentric reducer using CFD approach, 878-883”. 11th International Conference on Heat Transfer, Fluid Mechanics and Thermodynamics (20-23 July 2015, South Africa), 883 pp.

Daugherty, R. L. & J. B. Franzini, 1965. Fluid mechanics with engineering applications. (6th edition). NY: McGraw-Hill Book Company, 574 pp.

Deev, A. V., T. Rasheed, M. C. Welsh, M. M. K. Khan & M. G. Rasul, 2009. Measurement of instantaneous flow velocities in a concentric reducer using particle image velocimetry: Study of scale deposition. Experimental Thermal and Fluid Science, 33 (6): 1003-1011.

Demir, V., H. Yürdem, A. Yazgı & T. Günhan, 2019. Measurement and prediction of total friction losses in drip irrigation laterals with cylindrical integrated in-line drip emitters using CFD analysis method. Journal of Agricultural Sciences, 25 (3): 354-366. https://doi.org/10.15832/ankutbd.433830

Demir, V., H. Yürdem, A. Yazgı & T. Günhan, 2020. Determination of the hydraulic properties of a flat type drip emitter using computational fluid dynamics. Tarim Bilimleri Dergisi - Journal of Agricultural Sciences, 26 (2): 226-235. https://doi:10.15832/ankutbd.492686

Demir, V., H. Yürdem, A. Yazgı & T. Günhan, 2022. Mikro jet yağmurlama sulama başlığında akış özelliklerinin hesaplamalı akışkanlar dinamiği ile incelenmesi. Ege Univ. Ziraat Fak. Derg., 59 (1): 93-105, https://doi.org/10.20289/zfdergi.929494

Howell, T. A. & F. A. Barinas, 1980. Pressure losses across trickle irrigation fittings and emitters. Transactions of the ASAE, 23 (4): 928-933.

Idel'chik, I. E., 1960. Handbook of hydraulic resistance: Coefficients of local resistance and of friction. Israel Program for Scientific Translations, 517 pp.

Jivani, G. & K. Naik, 2019. CFD Simulation and analysis of fluid flow through concentric reducer pipe fitting. International Research Journal of Engineering and Technology, 9: 1071-1076.

Juana, L., L. Rodrı´guez-Sinobas & A. Losada, 2002. Determining minor head losses in drip irrigation laterals I: Methodology. Journal of Irrigation and Drainage Engineering, 128 (6): 376-384.

Munson, B. R., D. F. Young & T. H. Okiiski, 2002. Fundamentals of Fluid Mechanics (4th edition). Hoboken, NJ: John Wiley & Sons, Inc, 836 pp.

Narayane, M. A. V., M. V. C. Pathade & M. R. G. Telrandhe, 2014. CFD analysis of water flow through gradual contraction joint. International Journal of Engineering Research, 3 (6): 1579-1581.

Ntengwe, F., M. Chikwa & L. Witika, 2015. Evaluation of friction losses in pipes and fittings of process engineering plants. International Journal of Scientific and Technology Research, 4 (10): 330-336.

Palau-Salvador, G., J. Arviza-Valverde & V. F. Bralts, 2004. “Hydraulic flow behavior through an in-line emitter labyrinth using CFD techniques, 1-8”. Proceedings of the ASAE/CSAE Annual International Meeting (2024, Ottawa, Canada). ASABE Paper No. 042252, 8 pp.

Provenzano, G. & D. Pumo, 2004. Experimental analysis of local pressure losses for micro-irrigation laterals. Journal of Irrigation and Drainage Engineering, 130 (4): 318-324.

Rennels, D. C. & H. M. Hudson, 2012. Pipe flow: A practical and comprehensive guide. Hoboken, NJ: John Wiley & Sons, Inc, 289 pp.

Roul, M. K. & S. K. Dash, 2011. Two-phase pressure drop caused by sudden flow area contraction/expansion in small circular pipes. International Journal for Numerical Methods in Fluids, 66 (11): 1420-1446.

Saldivia, L. A., V. F. Bralts, W. H. Shayya & L. J. Segerlind, 1990. Analysis of sprinkler irrigation system components using the finite element method. Transactions of the ASAE, 33 (4): 1195-1202.

Satish, G., K. A. Kumar, V. V. Prasad & S. M. Pasha, 2013. Comparison of flow analysis of a sudden and gradual change of pipe diameter using fluent software. International Journal of Research in Engineering and Technology, 2: 41-45.

Tan, W. C., C. W. Chan, L. E. Aik & A. AnasRahman, 2013. “Scale deposition analysis of fluid flow characteristic in a concentric reducer using CFD approach, (1-9)”. Paper ID: P288. International Conference on Mechanical Engineering Research (ICMER2013), (1-3 July 2013, Bukit Gambang Resort City, Kuantan, Pahang, Malaysia), 539 pp.

TS, 2019. Polietilen (PE) borular-Mekanik boru bağlantı sistemlerinde basınç düşmesi-Deney metodu ve özellikler.TS 6694, Türk Standardları Enstitüsü, Ankara, 6 pp.

Wang, L. Y., Z. C. Zheng, Y. X. Wu, J. Guo, J. Zhang & C. Tang, 2009. Numerical and experimental study on liquid-solid flow in a hydrocyclone. Journal of Hydrodynamics, Ser B, 21 (3): 408-414. https://doi.org/10.1016/S10016058(08)60164-X

Wei, Q., Y. Shi, W. Dong, G. Lu & S. Huang, 2006. Study on hydraulic performance of drip emitters by computational fluid dynamics. Agricultural Water Management, 84 (1): 130-136. https://doi.org/10.1016/j.agwat.2006.01.016

White, F. M., 2001. Fluid Mechanics (4th edition). New York: McGraw-Hill, Inc, 826 pp.

Willmott, C. J. & K. Matsuura, 2005. Advantages of the mean absolute error (MAE) over the root mean square error (RMSE) in assessing average model performance. Climate Research, 30 (1): 79-82. https://doi.org/10.3354/cr030079

Willmott, C. J., S. G. Ackleson, R. E. Davis, J. J. Feddema, K. M. Klink, D. R. Legates, J. O'donnell & C. M. Rowe, 1985. Statistics for the evaluation and comparison of models. Journal of Geophysical Research: Oceans, 90: 8995-9005.

Zhang, J., W. Zhao, Z. Wei, Y. Tang & B. Lu, 2007. Numerical and experimental study on hydraulic performance of emitters with arc labyrinth channels. Computers and Electronics in Agriculture, 56 (2): 120-129.